Fusion of Multisensor Data: Review and Comparative Analysis

Uttam Kumar
Department of Management Studies & Centre for Sustainable Technologies, Indian Institute of Science, Bangalore, India.
e-mail: uttam@ces.iisc.ernet.in

Chiranjit Mukhopadhyay
Department of Management Studies, Indian Institute of Science, Bangalore, India.
e-mail: cm@mgmt.iisc.ernet.in

T. V. Ramachandra, *SM, IEEE*
Centre for Ecological Sciences & Centre for Sustainable Technologies, Indian Institute of Science, Bangalore, India.
e-mail: cestvr@ces.iisc.ernet.in

***Abstract*— Image fusion is a formal framework which is expressed as means and tools for the alliance of multisensor, multitemporal, and multiresolution data. Multisource data vary in spectral, spatial and temporal resolutions necessitating advanced analytical or numerical techniques for enhanced interpretation capabilities. This paper reviews seven pixel based image fusion techniques – intensity-hue-saturation, brovey, high pass filter (HPF), high pass modulation (HPM), principal component analysis, fourier transform and correspondence analysis. Validation of these techniques on IKONOS data (Panchromatic band at 1 m spatial resolution and Multispectral 4 bands at 4 m spatial resolution) reveal that HPF and HPM methods synthesises the images closest to those the corresponding multisensors would observe at the high resolution level.**

Keywords-multiresolution, multisensor, image fusion

I. INTRODUCTION

Earth observation satellites provide data covering different portions of the electromagnetic spectrum at different spatial, spectral and temporal resolutions. Satellites, such as QuickBird, IKONOS, IRS, bundle a 1:4 ratio of a high resolution (HR) panchromatic (PAN) band and low resolution (LR) Multispectral (MS) bands in order to support both spectral and best spatial resolutions while minimising on-board data handling needs [1]. Fusion of data from multiple sensors aids in delineating objects with comprehensive information due to the integration of spatial information present in the PAN image and spectral information present in the LR MS images. For example, fusion of 1 m IKONOS PAN image with 4 m MS images, permits identification of objects approximately one meter in length on the Earth's surface, especially useful in urban areas because the characteristic of urban objects are determined not only by their spectra but also by their structure. Remote sensing (RS) data fusion techniques integrate both PAN and MS data and can be performed at pixel [2], feature [3] and decision [4] levels. This paper reviews the outcome of seven pixel based image fusion techniques.

II. IMAGE FUSION TECHNIQUES

RS data are radiometrically and geometrically corrected (at pixel level) and georegistered considering the topographic undulations. For all methods discussed here, it is assumed that LR MS images are upsampled to the size of HR PAN image.

A. Intensity-Hue-Saturation (IHS)

In RGB – IHS algorithm, the LR MS data (DN^{l}_{MS1}, DN^{l}_{MS2}, DN^{l}_{MS3}) are transformed to the IHS (Intensity, Hue, Saturation) color space (equation 1) which separates the colour aspects in its average brightness (intensity). This corresponds to the surface roughness, its dominant wavelength contribution (hue) and its purity (saturation) [5]. V_1 and V_2 are the intermediate variables. I is replaced with HR image – $DN^{h'}_{PAN}$ and is contrast stretched to match the original PAN image. The fused images of HR are obtained by performing an inverse transformation (equation 2).

$$\begin{pmatrix} DN^{l}_{PAN} \\ V_1 \\ V_2 \end{pmatrix} = \begin{pmatrix} \frac{1}{3} & \frac{1}{3} & \frac{1}{3} \\ \frac{-1}{\sqrt{6}} & \frac{-1}{\sqrt{6}} & \frac{2}{\sqrt{6}} \\ \frac{1}{\sqrt{6}} & \frac{-1}{\sqrt{6}} & 0 \end{pmatrix} \begin{pmatrix} DN^{l}_{MS1} \\ DN^{l}_{MS2} \\ DN^{l}_{MS3} \end{pmatrix} \quad (1)$$

$$I = DN^{l}_{PAN} \quad H = \tan^{-1}\left(\frac{V_2}{V_1}\right) \quad S = \sqrt{V_1^2 + V_2^2}$$

Since the forward and backward transformations are linear, replacing V_1 and V_2 in equation (2) by V_1 and V_2 from (1) yields the mathematical model (equation 3) where $DN^{l}_{PAN} = (1/3)\,(DN^{l}_{MS1} + DN^{l}_{MS2} + DN^{l}_{MS3})$ and $DN^{h'}_{PAN}$ is DN^{h}_{PAN}, stretched to have same mean variance as DN^{l}_{PAN}.

$$\begin{pmatrix} DN^{h}_{MS1} \\ DN^{h}_{MS2} \\ DN^{h}_{MS3} \end{pmatrix} = \begin{pmatrix} 1 & \frac{-1}{\sqrt{6}} & \frac{3}{\sqrt{6}} \\ 1 & \frac{-1}{\sqrt{6}} & \frac{-3}{\sqrt{6}} \\ 1 & \frac{2}{\sqrt{6}} & 0 \end{pmatrix} \begin{pmatrix} DN^{h'}_{PAN} \\ V_1 \\ V_2 \end{pmatrix} \quad (2)$$

$$\begin{pmatrix} DN^{h}_{MS1} \\ DN^{h}_{MS2} \\ DN^{h}_{MS3} \end{pmatrix} = \begin{pmatrix} DN^{l}_{MS1} \\ DN^{l}_{MS2} \\ DN^{l}_{MS3} \end{pmatrix} + \left(DN^{h'}_{PAN} - DN^{l}_{PAN}\right) \begin{bmatrix} 1 \\ 1 \\ 1 \end{bmatrix} \quad (3)$$

978-0-7695-3571-5/09 $25.00 © 2009 IEEE
DOI 10.1109/GCIS.2009.457

B. Brovey Transform (BT)

BT is based on the chromaticity transform with a limitation that only three bands are involved [6]. It normalises the three MS bands used for RGB display and to multiply the result by any other desired data to add the intensity or brightness component to the image (equation 4) where $DN^{l}_{PAN} = (1/3)\,(DN^{l}_{MS1} + DN^{l}_{MS2} + DN^{l}_{MS3})$.

$$\begin{pmatrix} DN^{h}_{MS1} \\ DN^{h}_{MS2} \\ DN^{h}_{MS3} \end{pmatrix} = \begin{pmatrix} DN^{l}_{MS1} \\ DN^{l}_{MS2} \\ DN^{l}_{MS3} \end{pmatrix} + \left(DN^{h}_{PAN} - DN^{l}_{PAN}\right) \begin{bmatrix} \frac{DN^{l}_{MS1}}{DN^{l}_{PAN}} \\ \frac{DN^{l}_{MS2}}{DN^{l}_{PAN}} \\ \frac{DN^{l}_{MS3}}{DN^{l}_{PAN}} \end{bmatrix} \tag{4}$$

C. High pass filtering (HPF)

The high spatial resolution image is filtered with a small high-pass (HP) filter or taking the original HR PAN image and subtracting the LR PAN image, which is the low-pass (LP) filtered HR PAN image resulting in the high frequency part of the data which is related to the spatial information. This is pixel wise added to the LR bands. It preserves a high percentage of the spectral characteristics, since the spatial information is associated with the high-frequency information of the HR MS images, which is from the HR PAN image, and the spectral information is associated with the low-frequency information of the HR MS images, which is from the LR MS images (equation 5) [6].

$$DN^{h}_{MSS} = DN^{l}_{MS} + (DN^{h}_{PAN} - DN^{l}_{PAN}) \tag{5}$$

where $DN^{l}_{PAN} = DN^{h}_{PAN} * h_0$ and h_0 is a LP filter (average or smoothing filter).

D. High pass modulation (HPM)

This transfers the high frequency information of PAN to LR MS data, with modulation coefficients, which equal the ratio between the LR MS images and the LR PAN image [6] where $DN^{l}_{PAN} = DN^{h}_{PAN} * h_0$ and h_0 is the same LP filter as used in the HPF method.

$$DN^{h}_{MS} = DN^{l}_{MS} + (DN^{h}_{PAN} - DN^{l}_{PAN}) \frac{DN^{l}_{MS}}{DN^{l}_{PAN}} \tag{6}$$

E. Principal Component Analysis (PCA)

This transforms multivariate data into a data set of new un-correlated linear combinations of the original variables. It follows the idea similar to the IHS, of increasing the spatial resolution of MS images by introducing a HR PAN image, with the main advantage that an arbitrary number of bands can be used. The channel which will replace PC1 is stretched to the variance and average of PC1. The HR image replaces PC1 since it contains the information which is common to all bands while the spectral information is unique for each band. PC1 accounts for maximum variance which can maximise the effect of the HR data in the fused image. Finally, HR MS images are determined by performing the inverse PCA transform. The transformation matrix v contains the eigenvectors, ordered with respect to their eigenvalues. It is orthogonal and determined either from the covariance or correlation matrix of the input LR MS images [6].

$$\begin{bmatrix} PC1 \\ PC2 \\ \dots \\ PCn \end{bmatrix} = \begin{bmatrix} v11 & v21 & \dots & vn1 \\ v12 & v22 & \dots & vn2 \\ \dots & \dots & \dots & \dots \\ v1n & v2n & \dots & vnn \end{bmatrix} \begin{bmatrix} DN^{l}_{MS1} \\ DN^{l}_{MS2} \\ \dots \\ DN^{l}_{MSn} \end{bmatrix} \tag{7}$$

where the transformation matrix

$$v = \begin{bmatrix} v11 & v12 & \dots & v1n \\ v21 & v22 & \dots & v2n \\ \dots & \dots & \dots & \dots \\ vn1 & vn2 & \dots & vnn \end{bmatrix}$$

$$\begin{bmatrix} DN^{h}_{MS1} \\ DN^{h}_{MS2} \\ \dots \\ DN^{h}_{MSn} \end{bmatrix} = \begin{bmatrix} v11 & v12 & \dots & v1n \\ v21 & v22 & \dots & v2n \\ \dots & \dots & \dots & \dots \\ vn1 & vn2 & \dots & vnn \end{bmatrix} \begin{bmatrix} DN^{h'}_{PAN} \\ PC2 \\ \dots \\ PCn \end{bmatrix} \tag{8}$$

Similar to IHS method, equation 7 and 8 can be merged as follows:

$$\begin{bmatrix} DN^{h}_{MS1} \\ DN^{h}_{MS2} \\ \dots \\ DN^{h}_{MSn} \end{bmatrix} = \begin{bmatrix} DN^{l}_{MS1} \\ DN^{l}_{MS2} \\ \dots \\ DN^{l}_{MSn} \end{bmatrix} + (DN^{h'}_{PAN} - DN^{l}_{PAN}) \begin{bmatrix} v11 \\ v21 \\ \dots \\ vn1 \end{bmatrix} \tag{9}$$

where DN^{l}_{PAN} = PC1 and $DN^{h'}_{PAN}$ is DN^{l}_{PAN}, stretched to have same mean and variance as PC1.

F. Fourier transformation (FT)

FT or filter fusion transfers the high spatial frequency content of the HR image to the MS imagery by combining the LP filter version of the duplicated LR MS image and a HP filter version of the more highly resolved PAN [7]. This preserves a high percentage of the spectral characteristic, since the spectral information is associated with the low spatial frequencies of the MS imagery. The spatial resolution data is extracted by HP filtering the more highly resolved PAN band. The cut-off frequencies of the filters have to be chosen in such a way that the included data does not influence the spectra of the opposite data. A sensible value is the Nyquist frequency of the MS imagery. The fusion process is shown in equation (10) where FT denotes the Fourier transformation.

$$MS^{H}_{i} = FT^{-1}\{LPF\{FT(MS^{L}_{i})\} + HPF\{FT(PAN)\}\} \tag{10}$$

The usage of the spatial frequency domain is convenient

for the filter design and allows a faster computation for large imagery. After fusing both filtered spectra, the inverse Fourier transform (FT^{-1}) leads back into the image domain. The limitation of the approach is the introduction of false edges if the LR MS bands and the HR PAN exhibit a weak correlation.

G. Correspondence Analysis (CA)

Here, the data table (X) is transformed into a table of contributions of the Pearson chi-square statistic [1]. First, pixel (Xij) values are converted to proportions (Pij) by dividing each pixel (Xij) value by the sum (x++) of all pixels in data set. The result is a new data set of proportions (table Q), and the size is r x c. Row weight pi+ is equal to xi+/x++, where xi+ is the sum of values in row i. Vector [p+j] is of size c. The Pearson chi-square statistic, $\chi 2p$, is a sum of squared χij values computed for every cell 'ij' of the contingency table:

$$X_{ij} = \frac{O_{ij} - E_{ij}}{\sqrt{E_{ij}}} = \sqrt{x_{++}} \left[\frac{p_{ij} - p_{i+}p_{+j}}{\sqrt{p_{i+}p_{+j}}} \right] \quad (11)$$

If we use q_{ij} values instead of X_{ij} values, so that $q_{ij} = \chi_{ij} / \sqrt{\chi_{++}}$, eigenvalues will be smaller than or equal to 1 which is more convenient. We used the q_{ij} values to form matrix $\overline{Q}_{r \times c}$ which is

$$\overline{Q}_{r \times c} = \left[q_{ij} \right] = \left[\frac{p_{ij} - p_{i+}p_{+j}}{\sqrt{p_{i+}p_{+j}}} \right]. \quad (12)$$

After this point, the calculation of eigenvalues and the eigenvectors is similar to the PCA methods. Matrix U produced by

$$U_{c \times c} = \overline{Q}^{T}_{c \times r} \overline{Q}_{r \times c} \quad (13)$$

is similar to the covariance matrix of PCA. MS data are then transformed into the component space using the matrix of eigenvectors. A difference between CA and PCA fusion is the substitution of the last component with the high spatial resolution imagery as opposed to the substitution of the first component in the PCA. Two methods can be used in this part of the CA fusion process. The first is the substitution of the last component with PAN, which is stretched to have same range and variance with the last CA component. Second is the inclusion of details from the PAN band into the last component. Spatial details can be represented as the ratios of pixel values at the lower resolutions of the same imagery and can be included into the last component by

$$CA_{SimComp} = \frac{Pan_{High}}{Pan_{mean}} * CA_{LastComp} \quad (14)$$

where $CA_{SimpComp}$ is the new simulated last component image with the spatial resolution of Pan_{High} which is the high spatial resolution PAN image. Pan_{Mean} is the image with local mean values of Pan_{High} over neighbourhoods equivalent to footprints of $CA_{LastComp}$ image pixels. Noting that Pan_{Mean} can be calculated either by block averaging pixels within the footprints of the low spatial resolution image pixels, or using smoothing convolution filters [8] such as a LP filter so that values are calculated once for each LR pixel block as an average of the high spatial resolution pixels within the block. Finally, the components image is transformed back to the original image space using the inverse matrix of eigenvectors.

III. DATA ANALYSIS AND RESULTS

Validation of the techniques discussed above was done using IKONOS PAN (525.8 – 928.5 μm, 1 m, acquired on February 23, 2004) and 4 m resolution MS bands (Blue, Green, Red and NIR, acquired: November 24, 2004). The size of PAN and MS images, covering a portion of Bangalore city, India, is 1200 x 1600 and 300 x 400 respectively. The pairs of the images were geometrically registered and the LR images were upsampled to 1200 x 1600 by nearest neighbour algorithm. IKONOS data were collected at 11-bits per pixel (2048 gray tones). The processing and evaluation were based on the original 11-bit and the data were converted to 8-bit for display purpose only. Fig. 1 (1 and 2) shows the PAN image and the natural colour composite of the R-G-B combination resampled at 1 m pixel size. The study area is composed of various features such as buildings, race course, buses, parks, etc. ranging in size from 1 m to 100 m. The correlation coefficients (CCs) between PAN (downsampled to 4 m pixel size) and the original Blue band was 0.41, PAN and Green was 0.44, PAN and Red was 0.47 and PAN and NIR was 0.59. CC of the NIR band is higher than CCs of other bands, indicating that IKONOS NIR band is very important to the IKONOS PAN band. IHS and BT methods can handle only three bands so G-R-NIR combination was chosen for false colour composite (FCC). The resolution ratio between the IKONOS MS and PAN is 1:4, therefore, in the HPF and HPM methods, a 5 x 5 filter was used. The FCC of the G-R-NIR bands (at 1 m) and the fused result of the IHS, BT, HPF, HPM, PCA, FT and CA methods are displayed in Fig. 1 (3-10) respectively.

FT based fusion was performed in spectral domain as shown in Fig. 2. The aim of fusion here is to simulate MS data acquired at LR (4 m) to HR level (1 m), which is identical to MS images originally acquired at HR (1 m) had there been an ideal sensor that would acquire MS bands at 1 m. The performance of the techniques is evaluated in terms of the quality of synthesis of both spatial and spectral information. Visual inspection indicated that the spatial resolutions of the resultant images are higher than that of the original image as features (such as buses, trees, buildings, roads) which were not interpretable in the original image

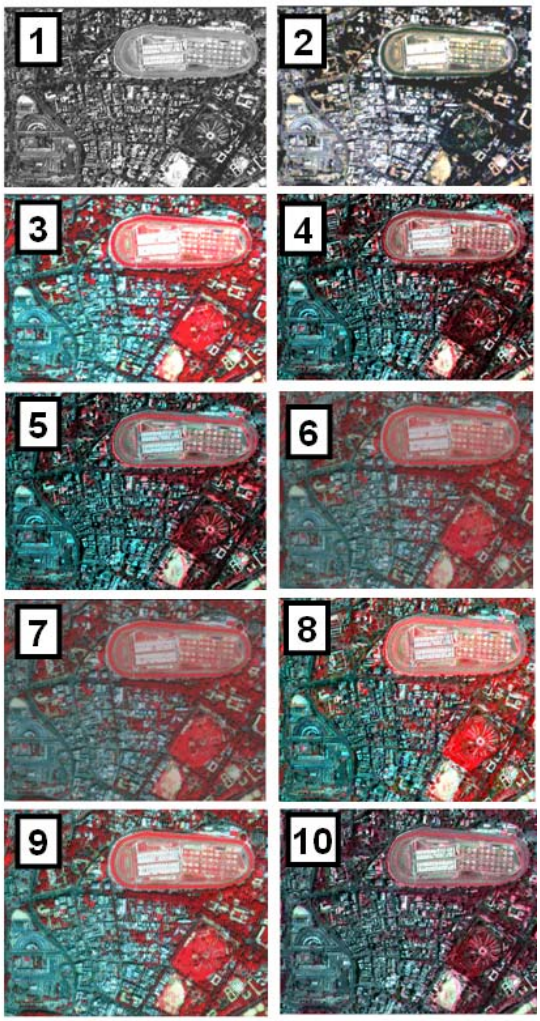

Figure 1. Original PAN image (1), original LR MS image (B-G-R) resampled at 1 m pixel size (2), original LR MS image (G-R-NIR) resampled at 1 m pixel size (3), Fusion through IHS (4), BT (5), HPF (6), HPM (7), PCA (8), FT (9) and CA (10).

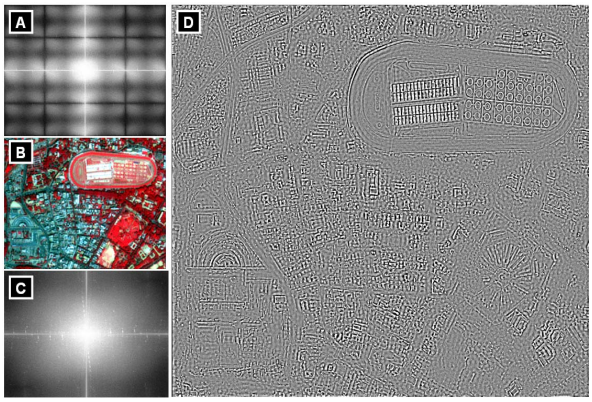

Figure 2. (A) FT on MS (B) Inverse FT on MS, (C) FT on PAN, (D) Inverse FT on PAN.

[Fig. 1 (3)] are identifiable in the resultant images [Fig. 1 (4-10)]. IHS, BT, and CA [Fig. 1 (4, 5 and 10)] produce significant color distortion, while HPF, HPM, PCA and FT methods [Fig. 1 (6, 7, 8 and 9)] produce slight colour distortion in buildings/builtup area. HPF, HPM and FT exhibit more sharpness. This is probably due to over-enhancement along the edge area because these additive methods have considered the differences in high-frequency information between the PAN and the MS bands. Overall, by visual inspection HPF, HPM, PCA and FT methods gives the synthesised result closest to what is expected with least colour distortion. The performance of these techniques were also analysed quantitatively by checking the CC that is often used as a similarity metric in image fusion. However, CC is insensitive to a constant gain and bias between two images and does not allow subtle discrimination of possible fusion artifacts. In addition, a universal image quality index (UIQI) [6] is used to measure the similarity between two images. UIQI is designed by modeling any image distortion as a combination of three factors: loss of correlation, radiometric distortion, and contrast distortion and is given by:

$$Q = \frac{\sigma_{\mathrm{AB}}}{\sigma_{\mathrm{A}}\sigma_{\mathrm{B}}} \cdot \frac{2\mu_A\mu_B}{\mu_A^2+\mu_B^2} \cdot \frac{2\sigma_A\sigma_B}{\sigma_A^2+\sigma_B^2} \qquad (15)$$

The first component is the CC for A (original MS band) and B (fused MS band). The second component measures how close the mean gray levels of A and B is, while the third measures the similarity between the contrasts of A and B. The dynamic range is [-1, 1]. If two images are identical, the similarity is maximal and equals 1. The synthesised HR MS images (1 m) are spatially degraded to the resolution level of the original LR MS images (4 m). UIQI are computed between the degraded HR MS images and the original LR MS images at the 4 m resolution level. Table 1 shows that the UIQI values of HPF and HPM are higher than the UIQI values of other methods. These two methods also showed higher scores in the NIR band. Since, PAN band includes the most important information from the NIR band (PAN and NIR exhibited highest correlation), therefore from the UIQI method, it is apparent that HPF is superior to all other methods but only slightly better than HPM, which is also reported in [6].

TABLE 1. UIQI OF FUSED AND ORIGINAL IMAGE

	Blue	Green	Red	NIR
HIS	-	0.17	0.27	0.12
BT	-	0.89	0.97	0.54
HPF	**0.85**	**0.94**	**0.96**	**0.98**
HPM	**0.83**	**0.94**	**0.97**	**0.95**
PCA	0.68	0.63	0.63	0.46
FT	0.43	0.22	0.73	0.81
CA	0.27	-0.01	0.06	-0.00

TABLE 2. CORRELATION BETWEEN IKONOS HR PAN AND CORRESPONDING LR PAN IMAGES FROM DIFFERENT METHODS

IHS	BT	HPF	HPM	PCA	FT	CA
0.32	0.32	**0.95**	**0.95**	0.32	-	0.27
p value for all CC = 2.2e-^{16}						
Both IHS and BT are limited to 3 bands (G, R and NIR). IHS and BT use the same low resolution PAN image. HPF and HPM use the same low resolution PAN image. There is no generation of low resolution PAN in FT.						

The closeness between two images was also quantified in terms of correlation function where each original IKONOS MS band was correlated with respect to each fused band obtained from the 7 techniques (except in IHS and BT where only three bands – G, R, and NIR were considered). Table 2 shows the correlation between the IKONOS HR PAN image and the corresponding LR PAN images by different methods (computed at 1 m pixel size). It can be seen from Table 1 and 2 that the degree of similarity between the HR PAN image and the LR PAN image correspond to the degree of spectral distortion of each band. The lower the similarity between the HR PAN image and the LR PAN image, the higher the spectral distortion and vice versa. HPF and HPM produce very high correlation of more than 0.9 with band 2, 3 and 4. BT has a high correlation in band 2 and 3. IHS and CA produce least correlation, while PCA and FT has medium correlation contrary to the earlier report in [1]. Statistical parameters – minimum, maximum and standard deviation were also used as a measure to examine the spectral information preservation for all the bands. HPM, HPF and PCA were closest to the minimum values of the original bands. For the maximum values, all bands from the HPF and HPM methods were very close to the maximum of original bands. All other methods induced changes in the maximum values in all the fused bands. The standard deviation values for the HPF, HPM, BT and PCA were similar to the original bands of the IKONOS. All other methods showed deviations. These parameters indicated that HPF and HPM are better compared to other methods, however, it could not clearly indicate which method among HPF and HPM is better since some values were closer to original bands in HPF while some were closer to original band values in HPM. By combining the visual inspection and the quantitative results, it was observed that the IHS, BT, and CA methods produce considerable spectral distortion, the FT and PCA methods produce slight spectral distortion and the HPF and HPM method produces the images closest to those the corresponding multisensors would observe at the HR level. However, if the contribution of the NIR band is considered in image fusion then HPF is slightly better than HPM.

IV. CONCLUSION

This paper reviews and analyses seven fusion techniques: IHS, BT, HPF, HPM, PCA, FT and CA. The performance of each method is determined by two factors: how the low resolution PAN image is computed and how the modulation coefficients are defined. If the low resolution PAN image is approximated from the low resolution MS image, it usually has a weak correlation with the high resolution PAN image, leading to color distortion in the fused image. If the low resolution PAN is a low-pass filtered high resolution PAN image, it usually shows less spectral distortion. If the modulation coefficient is set as a constant value, the reflectance differences between the PAN and the MS bands are unaccounted, and the fused images bias the color of the pixel toward the gray. By combination of the visual inspection results and the quantitative results, it is possible to see that the experimental results are in conformity with the theoretical analysis. HPF method followed by HPM produces the synthesised images closest to those the corresponding multi-sensors would observe at the high-resolution level.

ACKNOWLEDGMENT

We thank GeoEye Foundation, USA for providing IKONOS imagery for Greater Bangalore city. We are grateful to Indian Institute of Science for the financial assistance and infrastructure support.

REFERENCES

[1] H. I. Cakir, and S. Khorram, "Pixel Level Fusion of Panchromatic and Multispectral Images Based on Correspondence Analysis," Photogrammetric Engineering & Remote Sensing, vol. 74(2), 2008, pp. 183-192.

[2] P. Cheng, T. Toutin, and C. Pohl, "A comparison of geometric models for multisource data fusion," Proceedings of International Symposiumon Remote Sensing, GIS and GPS in Sustainable Development and Environmental Monitoring, GeoInformatics '95 - Hong Kong, 26-28 May 1995.

[3] M. Mangolini, "Apport de la fusion d'images satellitaires multicapteurs au niveau pixel en teÂ leÂ deÂ tection et photo-interpreÂtation," *Dissertation published at the University ofNice*, Sophia Antipolis, France, 15 November 1994.

[4] S. S. Shen, "Summary of types of data fusion methods utilized in workshop papers," *Multisource Data Integration in Remote Sensing, Proceedings of Workshop*, Maryland, U.S.A., 14-15 June 1990, NASA Conference Publication 3099 (Greenbelt, MD: NASA), pp. 145-149.

[5] W. J. Carper, T. M. Lillesand, and R. W. Kieffer, "The use of Intensity-Hue-Saturation transformations for merging SPOT Panchromatic and multispectral image Data," Photogrammetric Engineering and Remote Sensing, 56, 1990, pp. 459-467.

[6] Z. Wang, D. Ziou, C. Armenakis, D. Li, and Q. Li, "A Comparative Analysis of Image Fusion Methods," IEEE Transactions of Geoscience and Remote Sensing, vol. 43 (6), 2005, pp. 1391-1402.

[7] R. A. Schowengerdt, Remote sensing models and methods for image processing. Academic Press, San Diego, CA, USA, 1997.

[8] J. G. Liu, "Smoothing filter-based intensity modulation: A spectral preserve image fusion technique for improving spatial details," International Journal of Remote Sensing, 21(18), 2000, pp. 3461-3472.